Aqueous transfer of colloidal metal oxide nanocrystals *via* base-driven ligand exchange

Vikram S. Lakhanpal, Benjamin Z. Zydlewski, Xing Yee Gan, Hugo Celio, Huei-Ru "Molly" Jhong, Charles K. Ofosu, Delia J. Milliron*

Supporting Information

Table of Contents:

Methods....2
Synthesis of Metal Oxide NCs....2
Base Stripping of Metal Oxide NCs....3
Film Preparation....3
Characterization Methods....4
Surface Energy Calculations of Thin Films....4
XPS Analysis Methods....5
Supplementary Data....7
Additional CIO Characterization....7
Dispersion Pictures and Size Distributions....7
XRD....8
XPS....9
Characterization of other NC materials....11
STEM....11
Dispersion Pictures....12
Size Distributions....13
FTIR....14
DLS....15
Zeta Potential....16
XRD....17
XPS....18
Dispersion Spectra....26
Thin Film Characterization....27
References....29

Methods:

Synthesis of Metal Oxide NCs

Nanocrystals (NCs) were synthesized based on previously published methods. For Ce:InO_3 (5% doping), a 0.5 M metal-precursor solution was prepared using In (III) acetate (99.99%) and Ce (III) acetylacetonate hydrate, which were dissolved in oleic acid (90%) and stirred for 1 hour at 150°C under nitrogen flow. In a separate three-neck flask, oleyl alcohol (technical grade, 85%) was heated to 290°C. The precursor solution was then injected dropwise into the hot oleyl alcohol using a syringe pump at 0.2 mL/min. After injection of the precursor, the solution was cooled to room temperature. The NCs were then washed by repeated flocculation and dispersion with isopropyl alcohol and hexane, respectively.[1]

Undoped In_2O_3 NCs were synthesized by the same method, albeit with the cerium precursor replaced by a stoichiometrically equivalent amount of indium acetate. Sn:In_2O_3 (5% doping) was synthesized by a similar method as previously published, with Sn (IV) acetate as the dopant precursor.

CeO_2 was synthesized in a heat-up reaction, in which 2 mmol $Ce(NO_3)_3 \cdot 6H_2O$ was mixed with 24 mmol oleylamine and 5 mL squalane in a 50 mL round bottom flask under an inert nitrogen environment. The mixture was magnetically stirred at a constant speed, heated to 80°C, and mixed for 1 h to fully dissolve the reactants. The mixture was then heated to 120°C and degassed for 1 h to remove water from the flask. After degassing, the flask was placed under nitrogen again and heated to 250°C for 2 h for NCs nucleation and growth. After the reaction, 7.5 mL of toluene were added to the dispersion and the NCs were purified four times by flocculation with isopropanol (IPA), centrifugation, and redispersion with hexane.[2]

TiO_2 was synthesized in a hot injection reaction[3]. 8 mmol oleic acid, 104 mmol oleyl alcohol, and 32 mL octadecene were mixed in a 100 mL round bottom flask under vacuum at 120°C for 1.5 hours. After this, the flask was placed under nitrogen before 8 mmol of Ti (IV) ethoxide were injected and the reaction was heated to 290°C, where the reaction ran for 1 hour. After cooling, the resultant NCs were purified through standard flocculation with IPA, centrifugation, and redispersion with hexane.

Base Stripping of Metal Oxide Nanocrystals

A stock solution of 0.2 M potassium hydroxide in MilliQ UltraPure water was prepared, of which 10 mL were placed in a vial with a stirbar. 25 mg of CIO NCs were dispersed in 10 mL of hexane, which was added dropwise to the vial. The vial was placed on a stirplate to prevent buildup of NCs at the hexane-water interface. After 24 hours of stirring, the hexane layer was pipetted out of the vial. The aqueous NC dispersion was split between two spin dialysis centrifuge tubes. Centrifuge tube filters were made of cellulose with a molecular weight cutoff of 50 kDa. The vial was rinsed of any settled NCs with 10 mL of UltraPure water, which was then transferred into the dialysis tubes before centrifugation at 4500 RPM for 5 minutes. The concentrated dispersions were diluted with 10 mL UltraPure water and centrifuged again two more times before the concentrated NCs were combined and dispersed in 5 mL UltraPure water. UIO NCs were stripped using the same method, while ITO NCs were stirred for 28 hours to allow for complete transfer from the hexane phase, and TiO_2 NCs were stirred for 40 hours. CeO_2 NCs required a stronger basicity for ligand removal. 25 mL of 1M KOH were prepared and placed in a jar, while 25 mg of CeO_2 NCs were dispersed in 25 mL hexane and added dropwise to the jar. Instead of stirring, the jar was periodically swirled to dislodge NCs from the interface without creating an emulsion. CeO_2 NCs were fully transferred after 22 hours and purified in the same manner as the other ligand stripped NCs.

Film preparation

Glass substrates of 1.3 cm x 1.3 cm were cleaned via sonication for 20 minutes each in chloroform, acetone, and isopropanol, followed by 15 minutes cleaning using a UV ozone cleaner. Ligand capped NCs were spincoated out of hexane at a concentration of ~40 mg/mL. 50 μL were spincoated at 1000 RPM for 40 seconds followed by a drying step at 4000 RPM for 10 seconds. Ligand stripped NCs were spincoated out of water at ~40 mg/mL. 50 μL were spincoated at 800 RPM for 240 seconds followed by drying at 4000 RPM for 30 seconds. All films were dried at 150°C for 10 minutes and stored in a vacuum desiccator before conductivity and optical transmission measurements were performed. Profileometry measurements showed the thickness of the resultant films was comparable to those spincast from ligand capped NC dispersions of similar concentration (~100 nm thick).

Characterization Methods

a. Dilute NC samples were dropcast on TEM grids and stored under vacuum overnight to dry. Scanning transmission electron microscopy (STEM) was performed on these TEM grids with a Hitachi S-5500.

b. NC samples were dropcast onto silicon substrates (cleaned the same as glass for spincoating). Fourier-transform infrared (FTIR) spectroscopy was performed on these samples in transmission mode with a Bruker Vertex 70 spectrometer.

c. Dynamic light scattering (DLS) and zeta potential measurements of dilute NCs dispersions were taken in a Malvern Zetasizer Nano ZS. Ligand capped samples were measured in a quartz cuvette, while ligand stripped samples were measured in disposable plastic cuvettes.

d. To gather structural information, the NCs were precipitated and allowed to fully dry. X-ray diffraction (XRD) patterns were collected from the remaining powder using a Rigaku R-Axis Spider using Cu Kα radiation with a wavelength of 1.54 Å. Crystallite size along the [222] direction of CIO NCs were obtained using the Debye-Scherrer equation. Diffraction peak widths were corrected for instrumental broadening measured from a LaB_6 powder standard as previously discussed by Kim *et al*[4].

e. The samples dropcast on silicon were used for x-ray photoelectron spectroscopy (XPS) with a Kratos Axis Ultra DLD spectrometer with a monochromatic Al Kα source (1486.6 eV).

f. Conductivity measurements were taken on spincoated samples using an Ecopia Hall Effect measurement system (HMS-5000) in the 4-point probe Van der Pauw geometry.

g. UV-visible spectroscopy on films was performed with a fiber-optic coupled ASD Inc. PANalytical spectrometer. Transmission spectra were recorded at normal incidence to the film. All transmission measurements were referenced to a background of a bare glass substrate of the same thickness prepared in the same way as the sample substrates.

Surface Energy Calculations of Thin Films

Surface energy of the ITO films was determined by measuring contact angles for two different liquids on the films and calculating with the Owens-Wendt-Rabel-Kaelbel (OWRK) method as detailed by Annamalai *et al*[5,6]. In short, a linear relationship is established between the liquid's surface tension properties and a function of the contact angle, in which the slope and y-intercept are based on the polar (γ_{sv}^{P}) and dispersive (γ_{sv}^{D}) components of the surface free energy (γ_{sv}):

$$\frac{\gamma_{lv}(1+\cos\theta)}{2\sqrt{\gamma_{lv}^{D}}} = \sqrt{\gamma_{sv}^{P}}\sqrt{\frac{\gamma_{lv}^{P}}{\gamma_{lv}^{D}}} + \sqrt{\gamma_{sv}^{D}}$$

To obtain a regression for this relationship, contact angles are measured for water, which has a highly polar surface tension, and for diiodomethane, which has a highly dispersive surface tension.

XPS Analysis Methods

Oxygen 1s spectra were fit to 4 peaks. The low-energy peak was assigned to lattice oxygen for each metal oxide. Two peaks were assigned to carboxylate (532.4 eV) and hydroxyl (531.5) groups bound to the NC surface[7,8]. A fourth, intermediate peak for defect-adjacent oxygen (DAO) was added at 530.5 eV. [9,10]

Spectra for metal species involved fitting doublets that form due to spin-orbit splitting in the 2p and 3d orbitals. Three guiding principles were used for relating the peaks in a doublet. 1. The ratio of the area of the lower energy peak and area of the high energy peak are held constant (2:1 for 2p orbitals, 3:2 for 3d orbitals). 2. The full-width half maxima of the doublet peaks are equal (an exception is made for Ti 2p, which does not follow this rule). 3. The spacing between doublet peaks is constant for an element (7.6 eV for In 3d, 18.6 eV for Ce 3d, 8.4 eV for Sn 3d, and 5.7 eV for Ti 2p).

In CIO NCs, prominent changes are observed in the Ce 3d spectra after ligand stripping. The capped sample is fit to two doublets associated with Ce^{3+} oxidation state. Previous study of CIO NCs has shown *via* X-ray absorption spectroscopy (XAS) that while some Ce^{4+} is present in the CIO, Ce^{3+} is more common given the dopant occupies an In^{3+} lattice site[11]. Additionally, in XPS analysis, most of the Ce^{4+} peaks overlap with the Ce^{3+} peaks, making their presence harder to observe. After stripping however, a previously undetected peak emerges at 916.6 eV that is characteristic of Ce^{4+} state[12]. After fitting to this feature and its corresponding doublet, we calculate that 20% of the Ce ions are 4+. At the same time, the prevalence of Ce near the NC surface decreases from 5% to 3.8% relative to the total metal ion content.

In CeO_2 NCs, a large peak appears in the O 1s spectrum at 531.X eV after stripping. This peak is assigned to oxygens in carbonate. The appearance of a K 2p doublet in the C 1s spectrum after stripping suggests that potassium carbonate forms in a side reaction involving decomposition of oleate ligands[13].

Supplementary Data:

Figure S1. CIO NCs at the beginning of base stripping (left) and after stripping and purification (right).

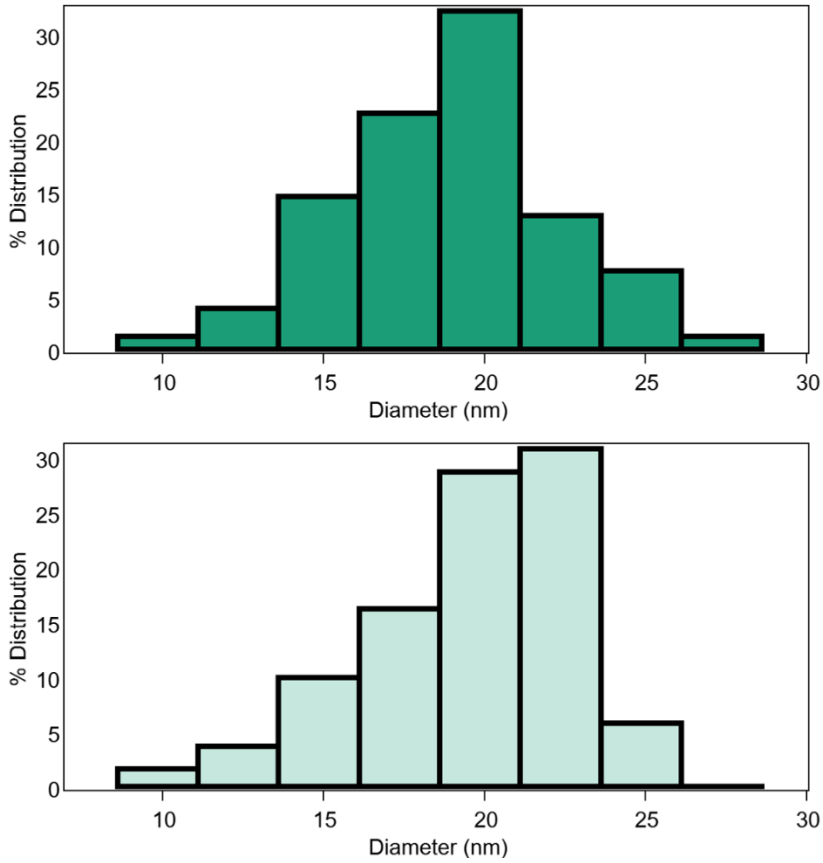

Figure S2. Size distribution for CIO-C (top) and CIO-S (bottom) based on STEM images in Figure 1a.

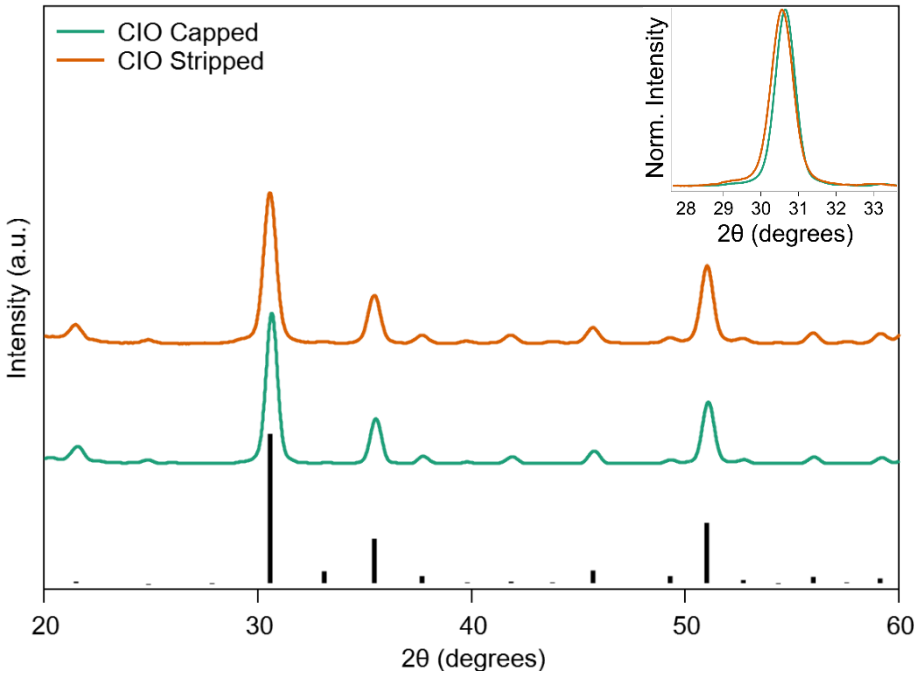

Figure S3. XRD patterns for CIO-C and CIO-S (offset for clarity) with the reference pattern for bixbyite (PDF# 96-101-0342), with normalized (222) peaks (inset).

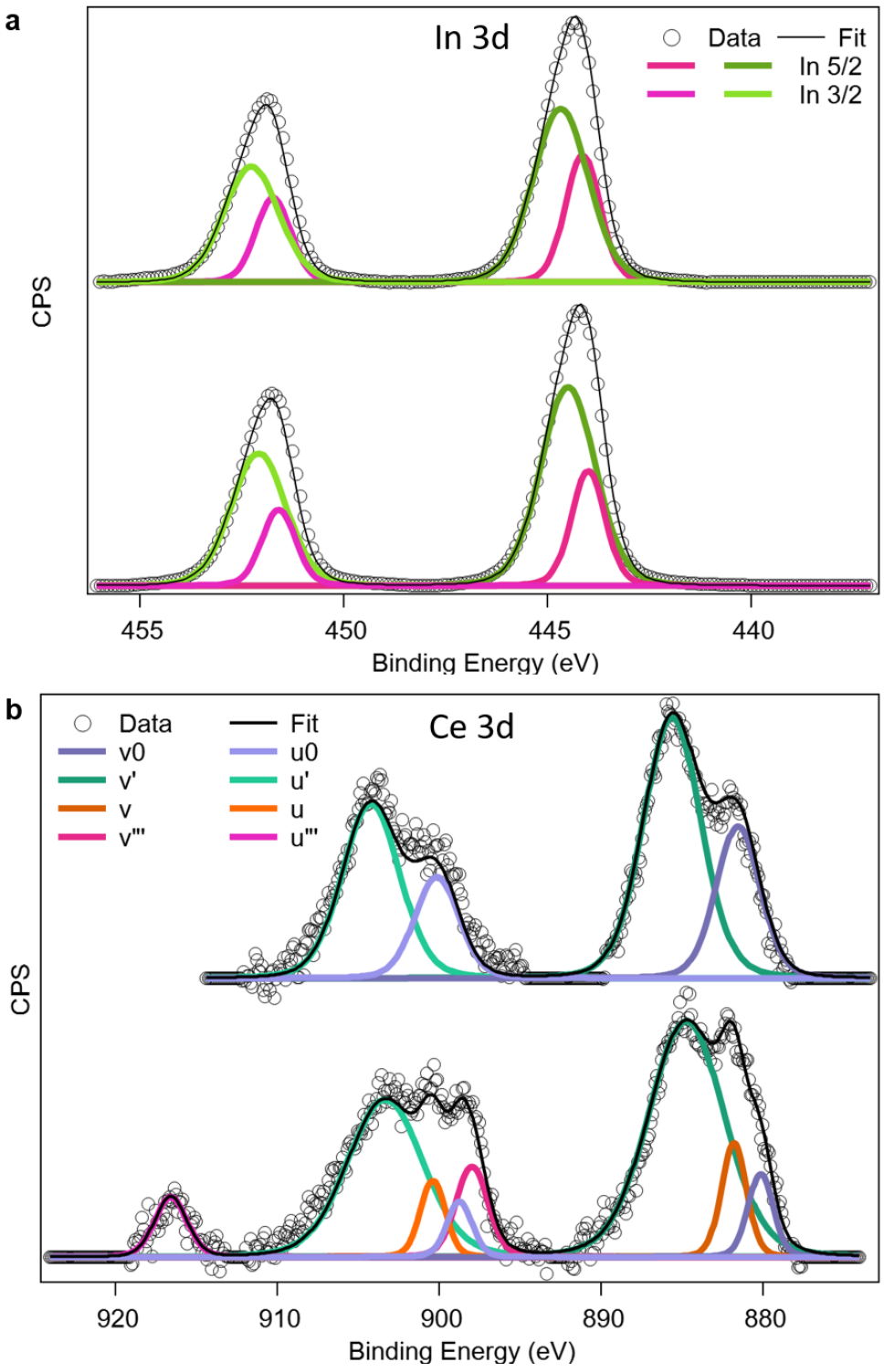

Figure S4. XPS of a) Indium 3d and b) Cerium 3d of ligand capped (tops) and ligand stripped (bottoms) CIO NCs. Orange and pink peaks (v, u, v”’, u”’) correspond to Ce^{4+}, while purple and green peaks (v0, u0, v’, and u’) correspond to Ce^{3+}.

Table S1. Positions and sizes of each peak in CIO-C and CIO-S XPS, normalized to the total indium peak intensity in their respective samples. Note that "Area" is calculated after factoring out the instrument's relative sensitivity factors for each element. Golden highlight is of lattice and defect adjacent oxygen peaks.

CIO-C				
Name	**Position**	**FWHM**	**Area**	**Area/Total In Area**
O 1s (Lattice)	529.88	1.14	24402	0.8374
O 1s (DAO)	530.73	0.98	4891	0.1680
O 1s (Hydroxyl)	531.55	1.27	9305	0.3193
O 1s (Carboxylate)	532.34	1.50	6125	0.2101
In 3d 5/2	444.13	0.88	3613	0.1239
In 3d 3/2	451.73	0.88	2402	0.0823
In 3d 5/2	444.60	1.60	13899	0.4770
In 3d 3/2	452.20	1.60	9239	0.3168
Ce 3d V0	885.68	4.14	483	0.0167
Ce 3d V'	904.28	4.14	321	0.0113
Ce 3d U0	881.56	3.22	219	0.0073
Ce 3d U'	900.16	3.22	146	0.0049

Ce doping:
3.86%

CIO-S				
Name	**Position**	**FWHM**	**Area**	**Area/Total In Area**
O 1s (Lattice)	529.78	1.17	24023	0.8590
O 1s (DAO)	530.65	1.37	5278	0.1888
O 1s (Hydroxyl)	531.48	1.50	9701	0.3471
O 1s (Carboxylate)	532.50	1.02	4044	0.1444
In 3d 5/2	444.00	0.88	3201	0.1143
In 3d 3/2	451.60	0.88	2131	0.0762
In 3d 5/2	444.46	1.57	13589	0.4860
In 3d 3/2	452.06	1.57	9047	0.3235
Ce 3d V0	880.38	2.04	60	0.0021
Ce 3d V'	884.72	5.44	384	0.0139
Ce 3d U0	898.98	2.04	40	0.0014
Ce 3d U'	903.32	5.44	257	0.0090
Ce 3d V	881.96	1.58	48	0.0017
Ce 3d V'''	897.99	2.28	61	0.0021
Ce 3d U	900.56	1.58	32	0.0010
Ce 3d U'''	916.59	2.28	41	0.0014

Ce^{3+}/Total Ce:
80.21%

Ce doping:
3.19%

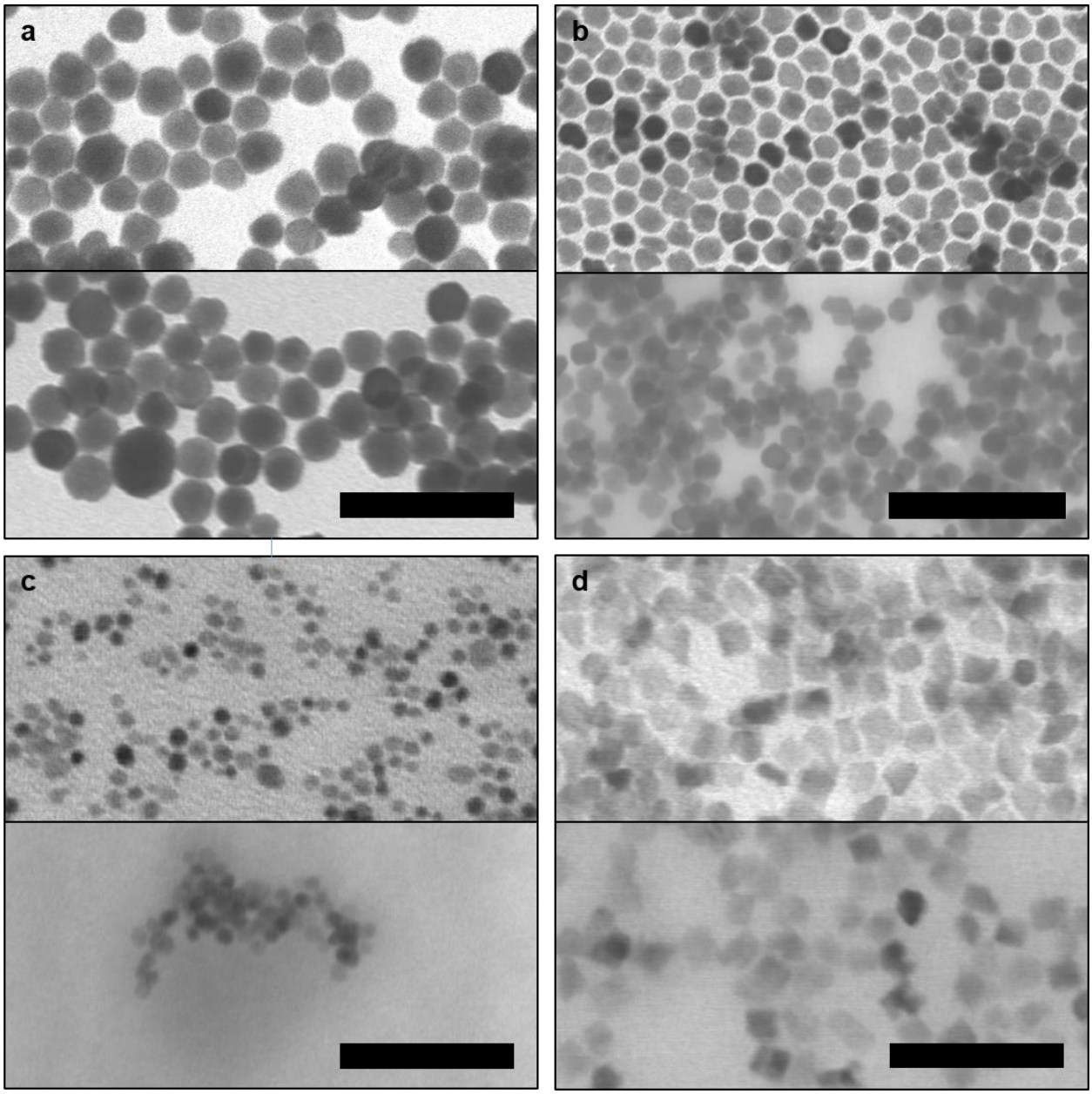

Figure S5. STEM taken before (tops) and after (bottoms) ligand stripping of a) undoped indium oxide (UIO), b) tin-doped indium oxide (ITO), c) cerium oxide (CeO_2), and d) titanium oxide (TiO_2) NCs. Scale bars are 100 nm (a, b) and 50 nm (c, d).

Figure S6. a) Ligand capped dispersions of (left to right), TiO_2, ITO, CIO, CeO_2, UIO. Aqueous ligand stripped dispersions of b) TiO_2 and c) ITO.

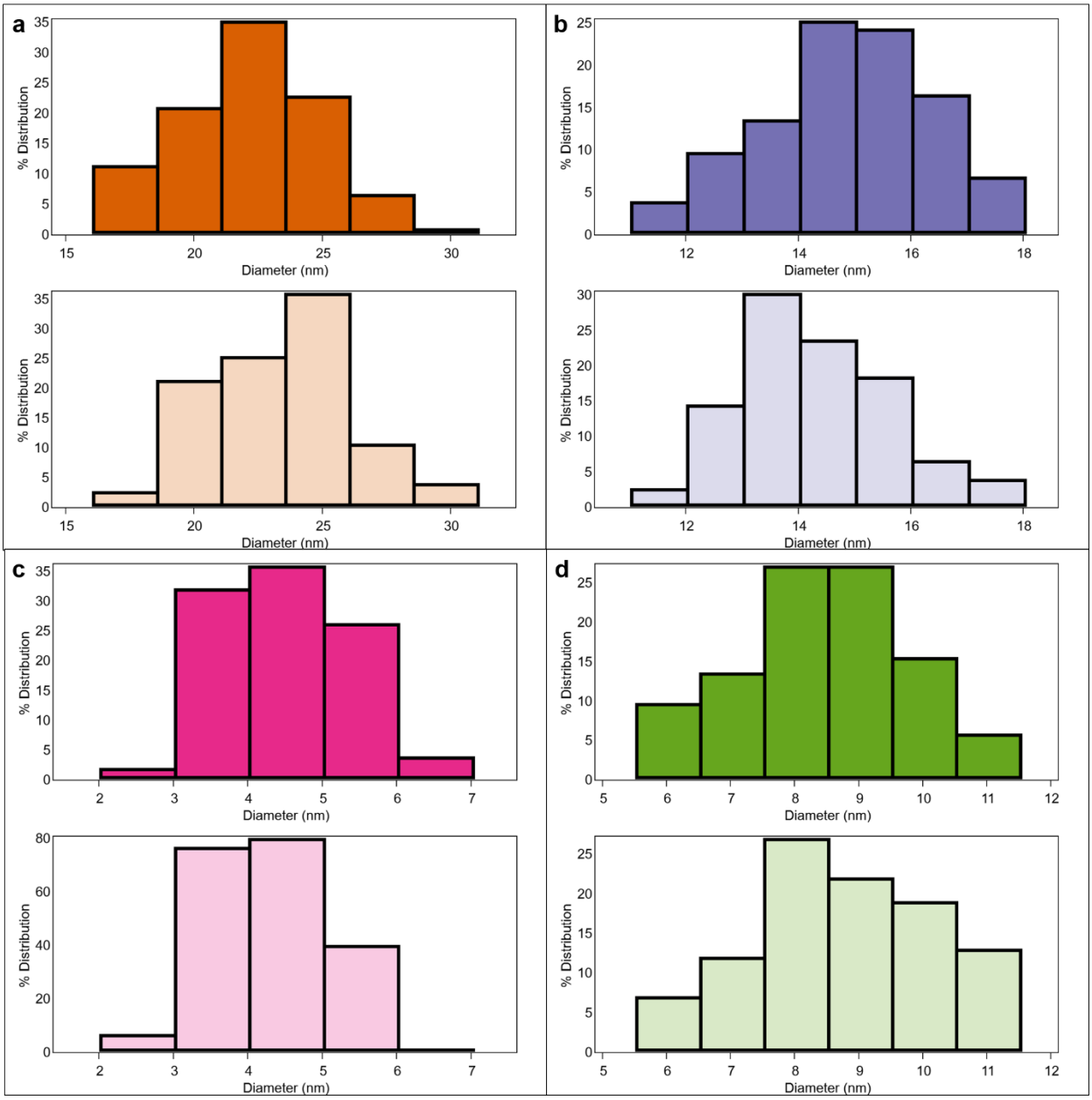

Figure S7. Size distributions for ligand capped (tops) and ligand stripped (bottoms) NCs based on STEM images for a) UIO, b) ITO, c) CeO_2, d) TiO_2

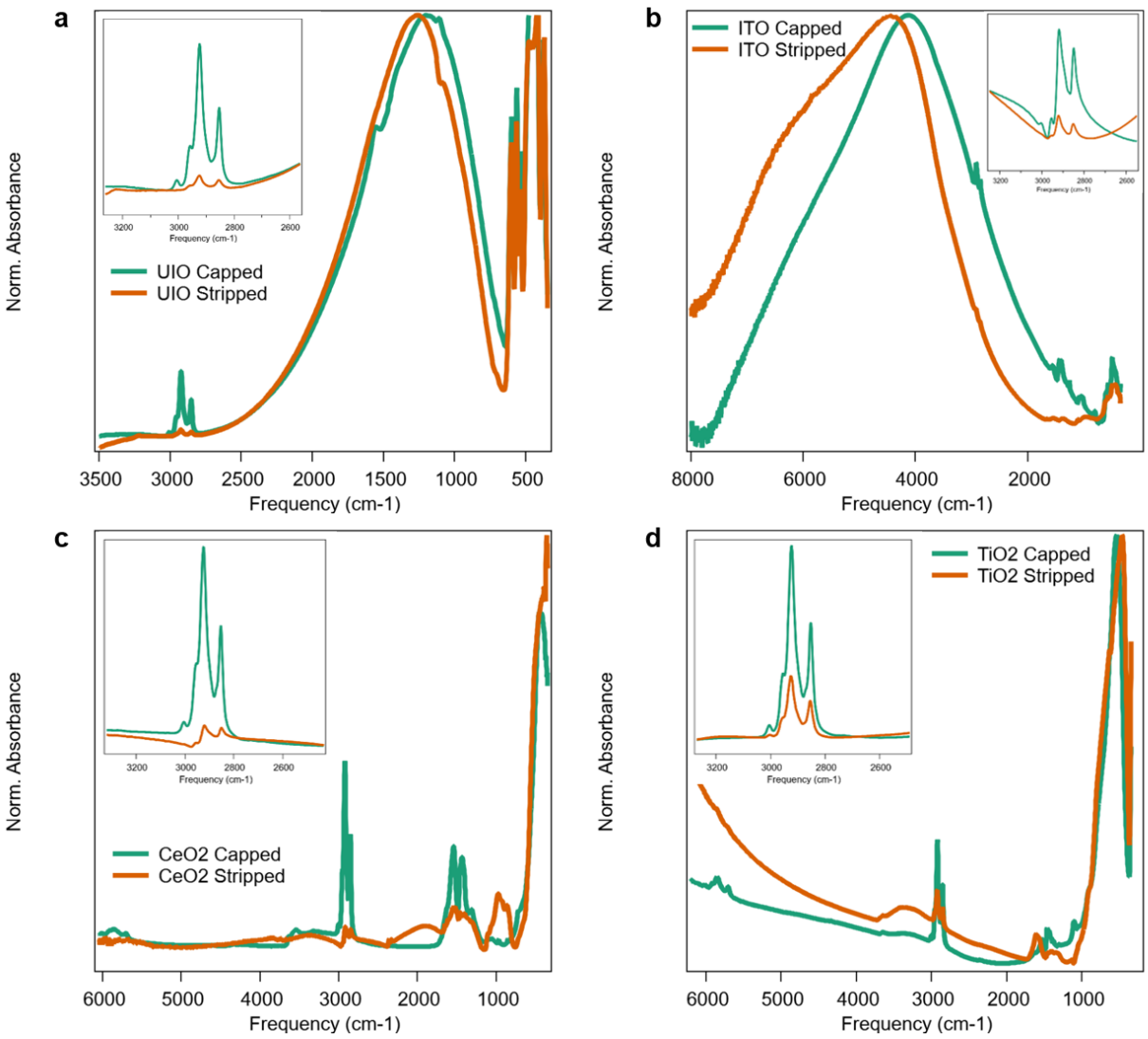

Figure S8. FTIR spectra of a) UIO, b) ITO, c) CeO_2, d) TiO_2 NCs before and after ligand stripping. UIO and ITO spectra sere normalized to the LSPR peak, while CeO_2 was normalized to a Ce-O feature at 454 cm^{-1} and TiO_2 was normalized to a Ti-O peak observed between 450 and 550 cm^{-1}. Insets show the decrease in the C-H stretching peaks between 2800 and 3100 cm^{-1} associated with oleate ligands. For ITO and TiO_2 spectra, linear baselines were fitted between 2600 and 3200 cm^{-1} and subtracted to isolate the C-H peaks.

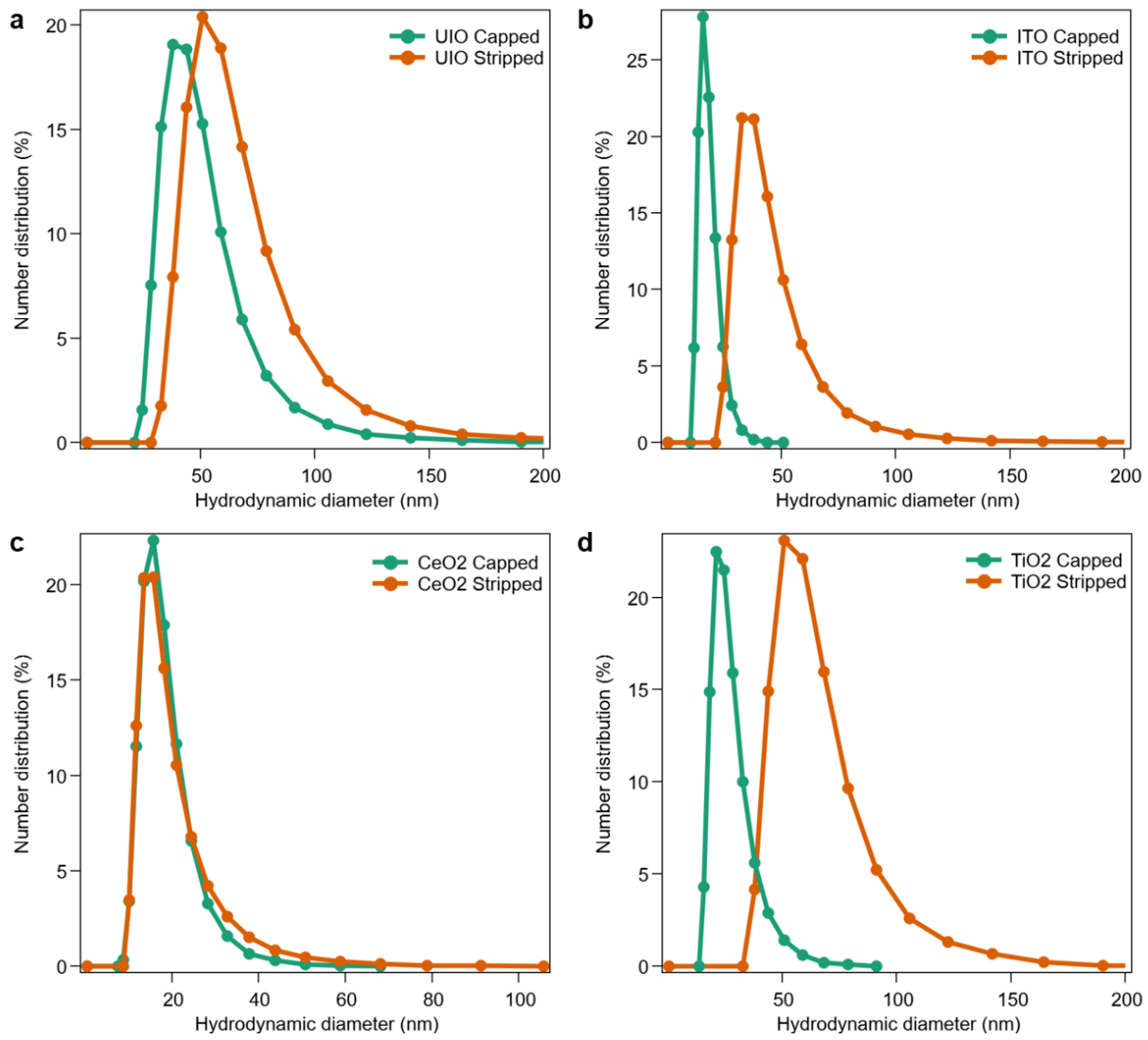

Figure S9. DLS of a) UIO, b) ITO, c) CeO_2, and d) TiO_2 NCs before and after ligand stripping.

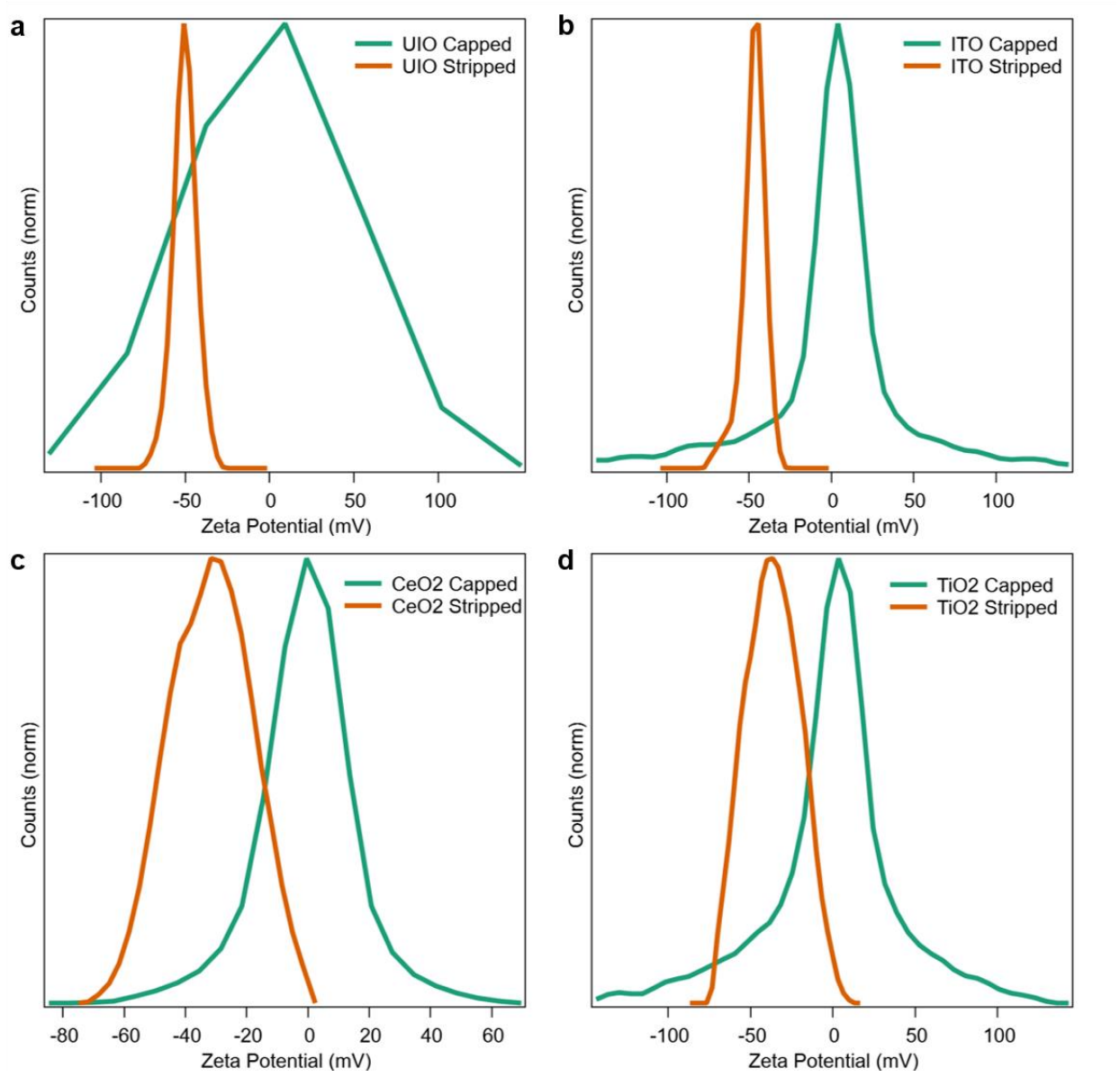

Figure S10. Zeta Potential of a) UIO, b) ITO, c) CeO_2, and d) TiO_2 NCs before and after ligand stripping.

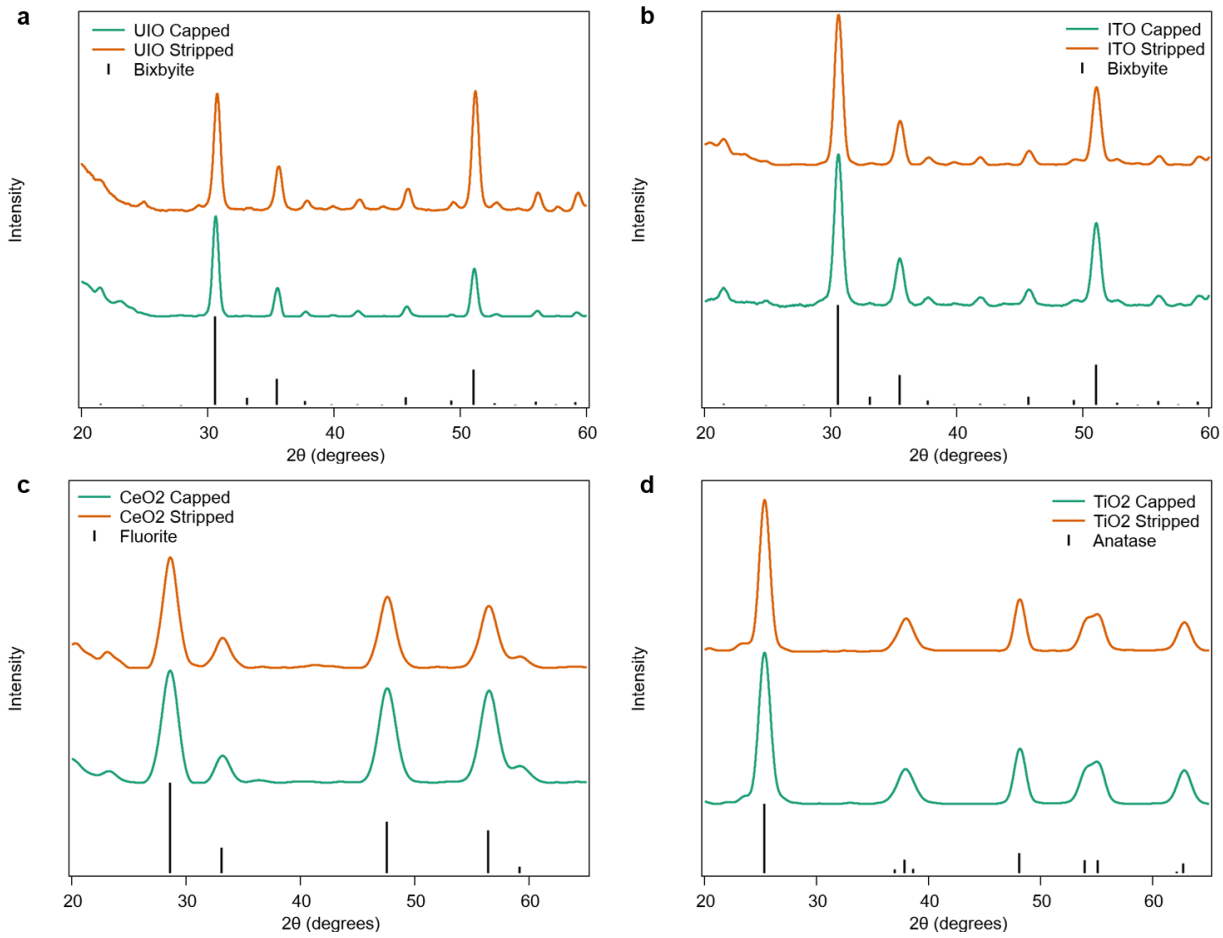

Figure S11. XRD patterns of a) UIO, b) ITO, c) CeO_2, and d) TiO_2 NCs before and after ligand stripping. Reference peaks for each material's crystal structure are also included: bixbyite (PDF# 96-101-0342) for UIO and ITO, fluorite (PDF# 96-434-3162) for CeO_2, and anatase (PDF# 96-900-9087) for TiO_2.

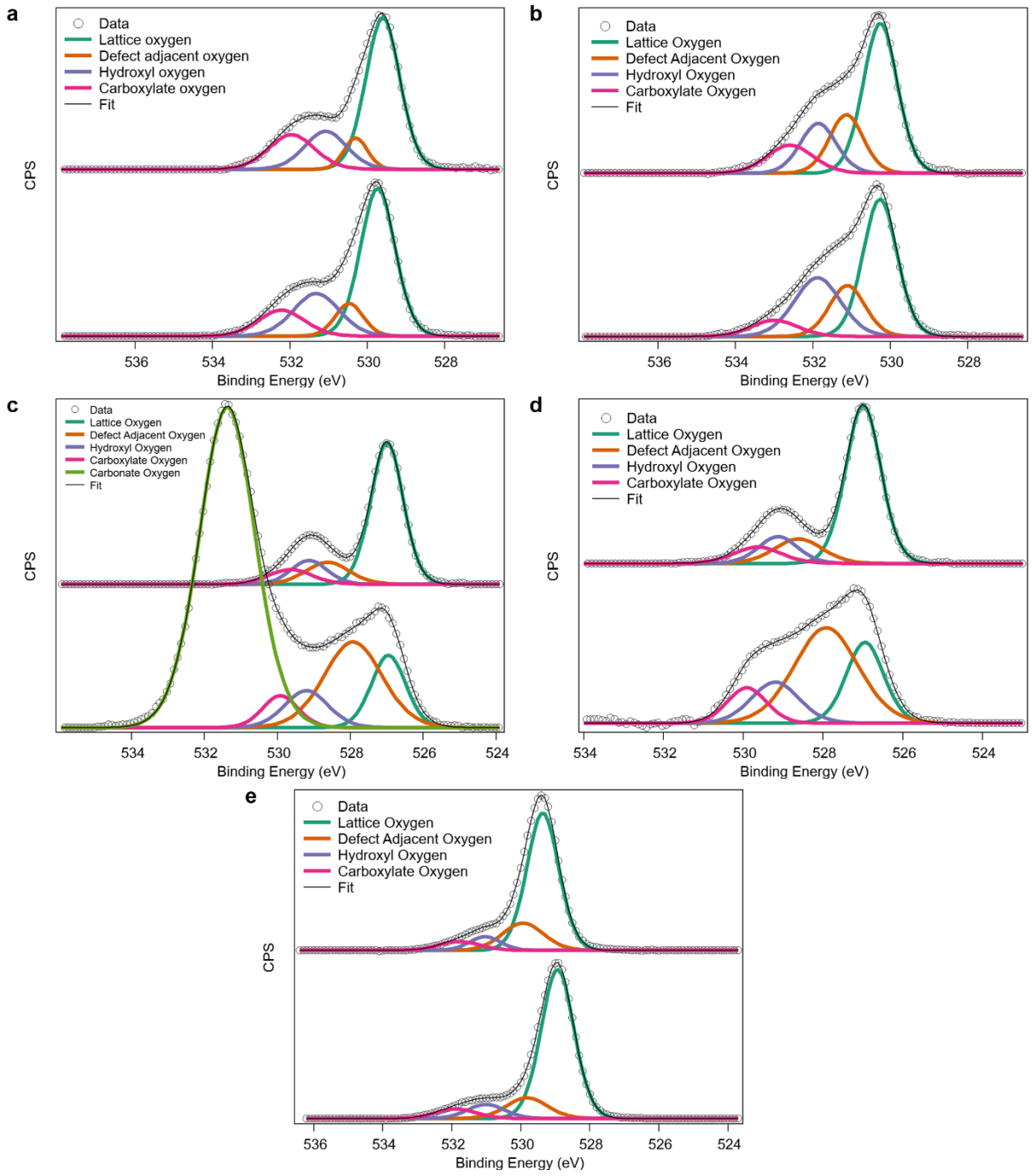

Figure S12. XPS of oxygen 1s in a) UIO, b) ITO, c) CeO_2, and e) TiO_2 before (tops) and after (bottoms) ligand stripping. d) CeO_2 O1s specta with the peak assigned to potassium carbonate subtracted.

Table S2. Details of XPS peak assignments for O 1s spectra for UIO, ITO, CeO_2, and TiO_2 NCs before and after ligand stripping.

UIO-C				
Name	**Position**	**FWHM**	**Area**	**Area/Total In Area**
O 1s (Lattice)	529.60	1.03	28544	0.7612
O 1s (DAO)	530.30	0.71	4075	0.1087
O 1s (Hydroxyl)	531.08	1.28	8886	0.2370
O 1s (Carboxylate)	531.96	1.40	8821	0.2352
In 3d 5/2	443.85	0.87	5303	0.1414
In 3d 5/2	444.38	1.61	17223	0.4594
In 3d 3/2	451.45	0.87	3525	0.0938
In 3d 3/2	451.98	1.61	11448	0.3054

UIO-S				
Name	**Position**	**FWHM**	**Area**	**Area/Total In Area**
O 1s (Lattice)	529.74	1.04	40217	0.7871
O 1s (DAO)	530.48	0.85	7228	0.1415
O 1s (Hydroxyl)	531.33	1.40	15506	0.3033
O 1s (Carboxylate)	532.23	1.40	9437	0.1848
In 3d 5/2	444.00	0.88	7244	0.1418
In 3d 5/2	444.50	1.58	23456	0.4590
In 3d 3/2	451.60	0.88	4815	0.0941
In 3d 3/2	452.10	1.58	15591	0.3050

ITO-C				
Name	**Position**	**FWHM**	**Area**	**Area/Total In Area**
O 1s (Lattice)	530.11	1.03	27841	0.7489
O 1s (DAO)	530.98	1.03	10831	0.2914
O 1s (Hydroxyl)	531.70	1.09	9776	0.2628
O 1s (Carboxylate)	532.43	1.40	7056	0.1896
Sn 3d 5/2	486.39	0.91	423	0.0113
Sn 3d 5/2	487.03	1.87	1262	0.0338
Sn 3d 3/2	494.79	0.91	282	0.0075
Sn 3d 3/2	495.43	1.87	841	0.0225
In 3d 5/2	444.35	0.81	6976	0.1877
In 3d 5/2	445.01	1.85	15350	0.4130
In 3d 3/2	451.95	0.81	4637	0.1248
In 3d 3/2	452.61	1.85	10203	0.2745

Sn doping: 7.02%

ITO-S				
Name	**Position**	**FWHM**	**Area**	**Area/Total In Area**
O 1s (Lattice)	530.11	1.03	36465	0.7400
O 1s (DAO)	530.96	1.08	14135	0.2867
O 1s (Hydroxyl)	531.72	1.40	21110	0.4283
O 1s (Carboxylate)	532.83	1.40	5795	0.1177
Sn 3d 5/2	486.40	0.89	529	0.0109
Sn 3d 5/2	487.11	1.83	1466	0.0297
Sn 3d 3/2	494.80	0.89	352	0.0072
Sn 3d 3/2	495.51	1.83	977	0.0199
In 3d 5/2	444.37	0.80	8787	0.1781
In 3d 5/2	445.03	1.85	20831	0.4225
In 3d 3/2	451.97	0.80	5841	0.1184
In 3d 3/2	452.63	1.85	13847	0.2810

Sn doping:
6.31%

CeO2-C				
Name	**Position**	**FWHM**	**Area**	**Area/Total Ce Area**
O 1s (Lattice)	529.36	1.03	27074	1.2386
O 1s (DAO)	530.99	1.40	5676	0.2593
O 1s (Hydroxyl)	531.49	1.16	5088	0.2329
O 1s (Carboxylate)	532.01	1.40	3785	0.1729
Ce 3d V0	880.14	1.45	359	0.0164
Ce 3d V'	883.98	4.08	4089	0.1871
Ce 3d U0	898.74	1.45	239	0.0107
Ce 3d U'	902.58	4.08	2723	0.1243
Ce 3d V	882.11	1.48	2058	0.0943
Ce 3d V"	888.57	4.39	3137	0.1436
Ce 3d V"'	898.10	2.24	3481	0.1593
Ce 3d U	900.71	1.48	1371	0.0629
Ce 3d U"	907.17	4.39	2089	0.0957
Ce 3d U"'	916.70	2.24	2318	0.1057

Ce^{3+}/Total Ce:
33.90%

CeO2-S				
Name	**Position**	**FWHM**	**Area**	**Area/Total Ce Area**
O 1s (Lattice)	528.24	1.29	5621	1.0764
O 1s (DAO)	529.20	1.02	2110	0.4035
O 1s (Hydroxyl)	529.89	1.06	1780	0.3401
O 1s (Carboxylate)	530.80	1.38	3101	0.5937
O 1s (Carbonate)	532.52	1.79	21832	4.1787
Ce 3d V0	880.92	1.11	87	0.0173
Ce 3d V'	884.44	3.02	331	0.0634
Ce 3d U0	899.52	1.11	58	0.0115
Ce 3d U'	903.04	3.02	221	0.0418
Ce 3d V	881.70	3.12	1043	0.2003
Ce 3d V"	887.73	4.28	750	0.1441
Ce 3d V"'	897.23	2.67	914	0.1744
Ce 3d U	900.30	3.12	697	0.1340
Ce 3d U"	906.33	4.28	501	0.0965
Ce 3d U"'	915.83	2.67	611	0.1167

Ce^{3+}/Total Ce:
13.38%

TiO2-C				
Name	**Position**	**FWHM**	**Area**	**Area/Total Ti Area**
O 1s (Lattice)	529.83	1.09	23604	1.7374
O 1s (DAO)	530.40	1.40	6043	0.4445
O 1s (Hydroxyl)	531.50	1.07	2310	0.1702
O 1s (Carboxylate)	532.25	1.40	1966	0.1447
Ti 2p 3/2	458.69	1.03	9060	0.6671
Ti 2p 1/2	464.39	2.00	4525	0.3329

TiO2-S				
Name	**Position**	**FWHM**	**Area**	**Area/Total Ti Area**
O 1s (Lattice)	529.41	1.12	37499	1.9421
O 1s (DAO)	531.48	1.27	4022	0.2082
O 1s (Hydroxyl)	530.29	1.40	6565	0.3398
O 1s (Carboxylate)	532.36	1.40	3029	0.1571
Ti 2p 3/2	458.22	1.03	12881	0.6670
Ti 2p 1/2	463.92	2.01	6434	0.3330

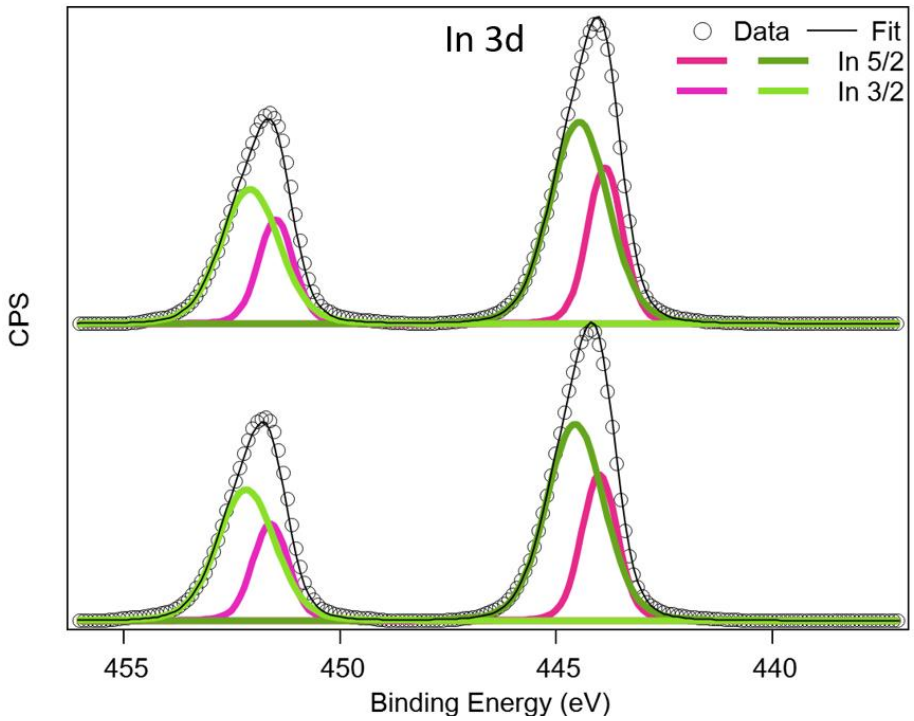

Figure S13. XPS of Indium 3d in ligand capped (top) and ligand stripped (bottom) UIO NCs.

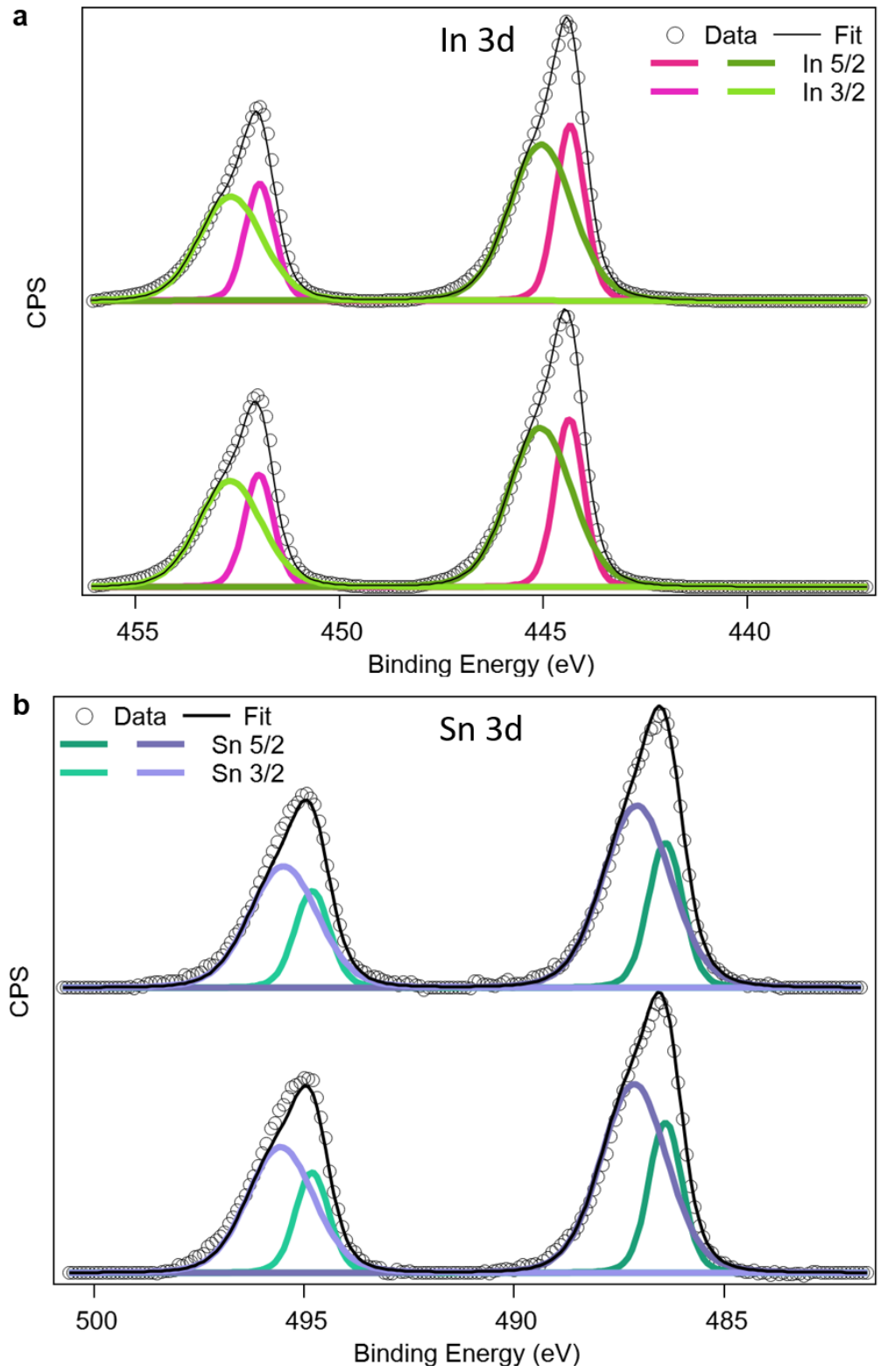

Figure S14. XPS of a) Indium 3d and b) Tin 3d of ligand capped (tops) and ligand stripped (bottoms) ITO NCs.

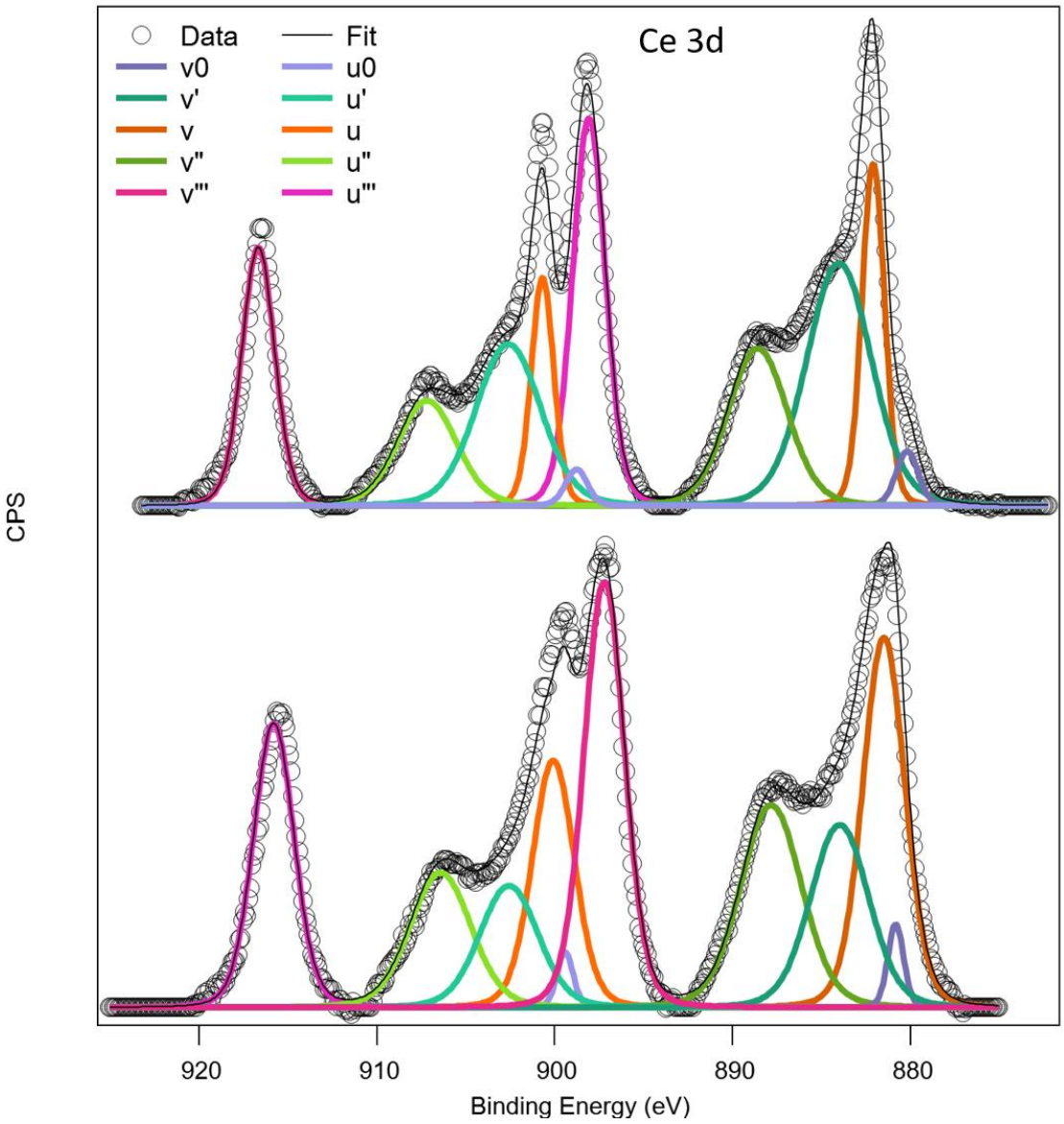

Figure S15. XPS of cerium 3d for ligand capped (top) and ligand stripped (bottom) CeO_2 NCs. Peaks v0, v', u0, and u' correspond to Ce^{3+}, while peaks v, v'', v''', u, u'', and u''' correspond to Ce^{4+}.

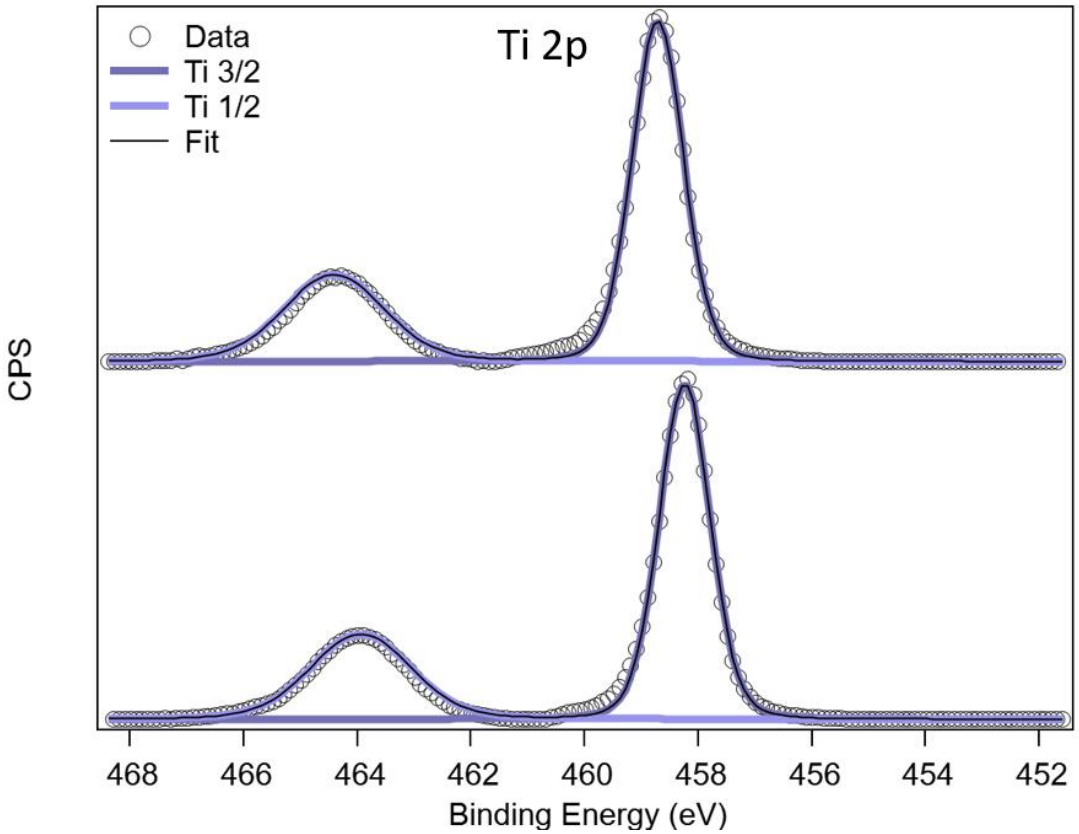

Figure S16. XPS of titanium 2p for ligand capped (top) and ligand stripped (bottom) TiO_2 NCs.

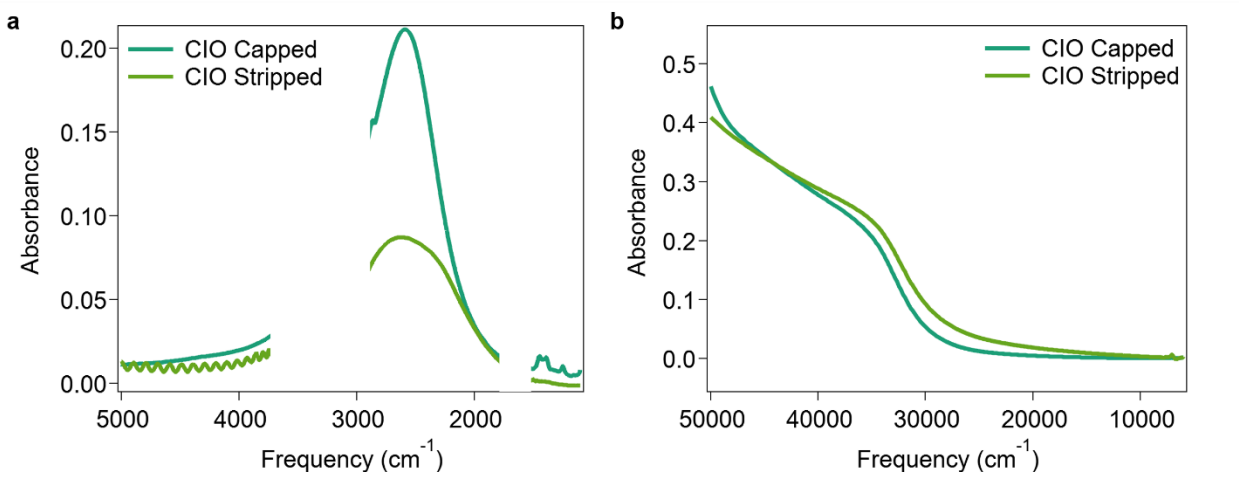

Figure S17. Changes in optical properties of CIO NCs before and after ligand stripping. a) LSPR as measured with FTIR spectroscopy. b) Band edge as measured with UV-Visible transmission spectroscopy. Capped particles are dispersed in tetrachloroethylene (TCE), stripped particles are dispersed in water. FTIR measurements were performed at 5 mg/mL in a liquid cell with a 0.025 μm pathlength, UV-Visible measurements were performed at 0.25 mg/mL in a quartz cuvette with a 1 mm pathlength.

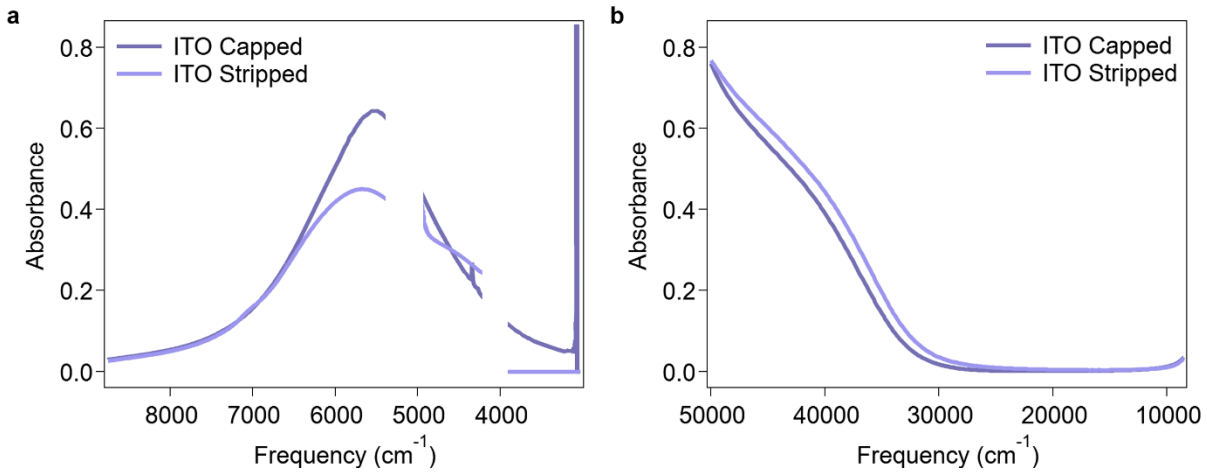

Figure S18. Changes in a) LSPR and b) band edge of ITO NCs before and after ligand stripping measured with UV-Visible light spectroscopy. Capped particles are dispersed in TCE, stripped particles are dispersed in water. Measurements were performed in a quartz cuvette with a 1 mm pathlength at 0.25 mg/mL

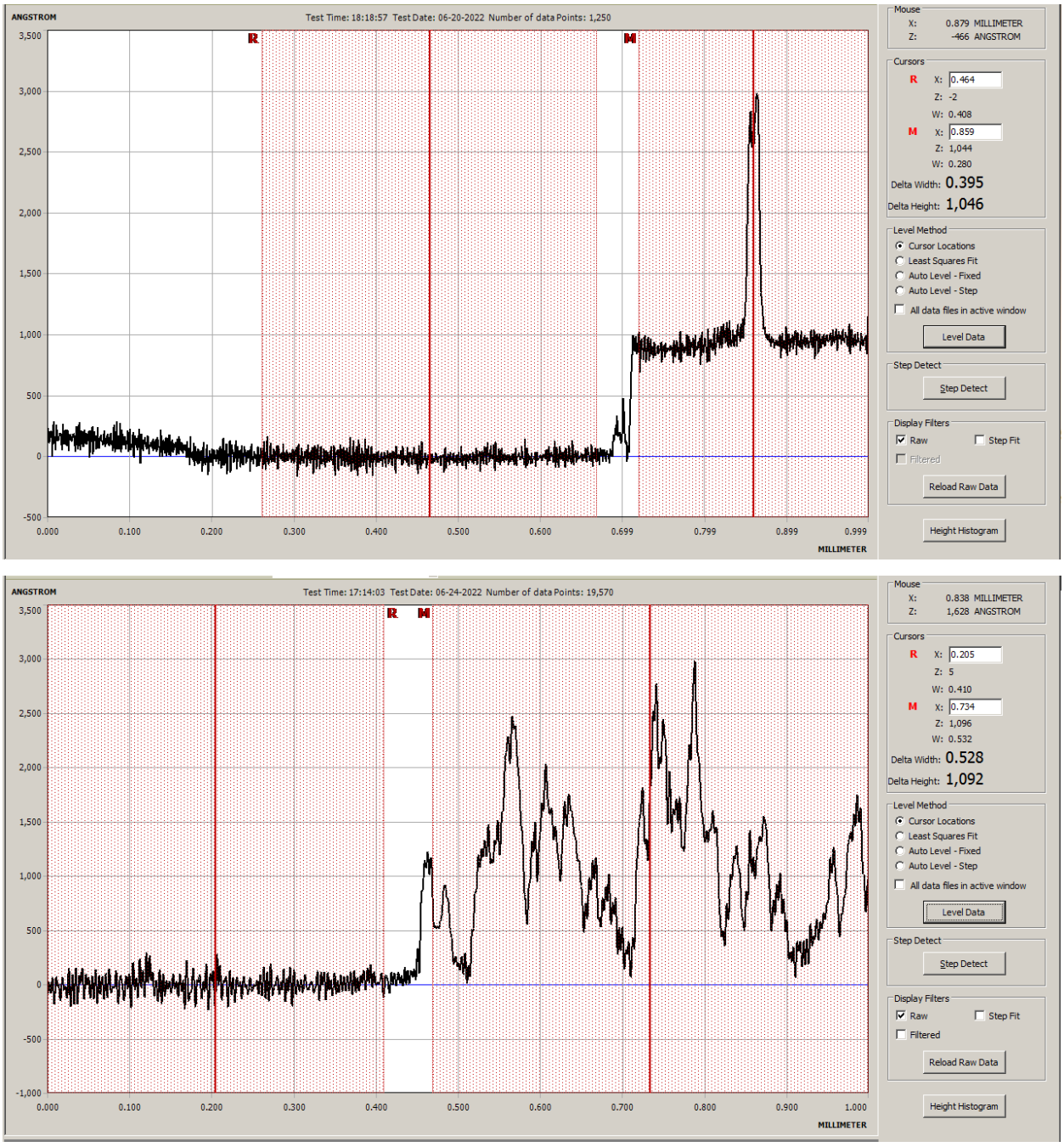

Figure S19. Profileometry measurements of thickness of ITO-C film (top) and ITO-S film (bottom).

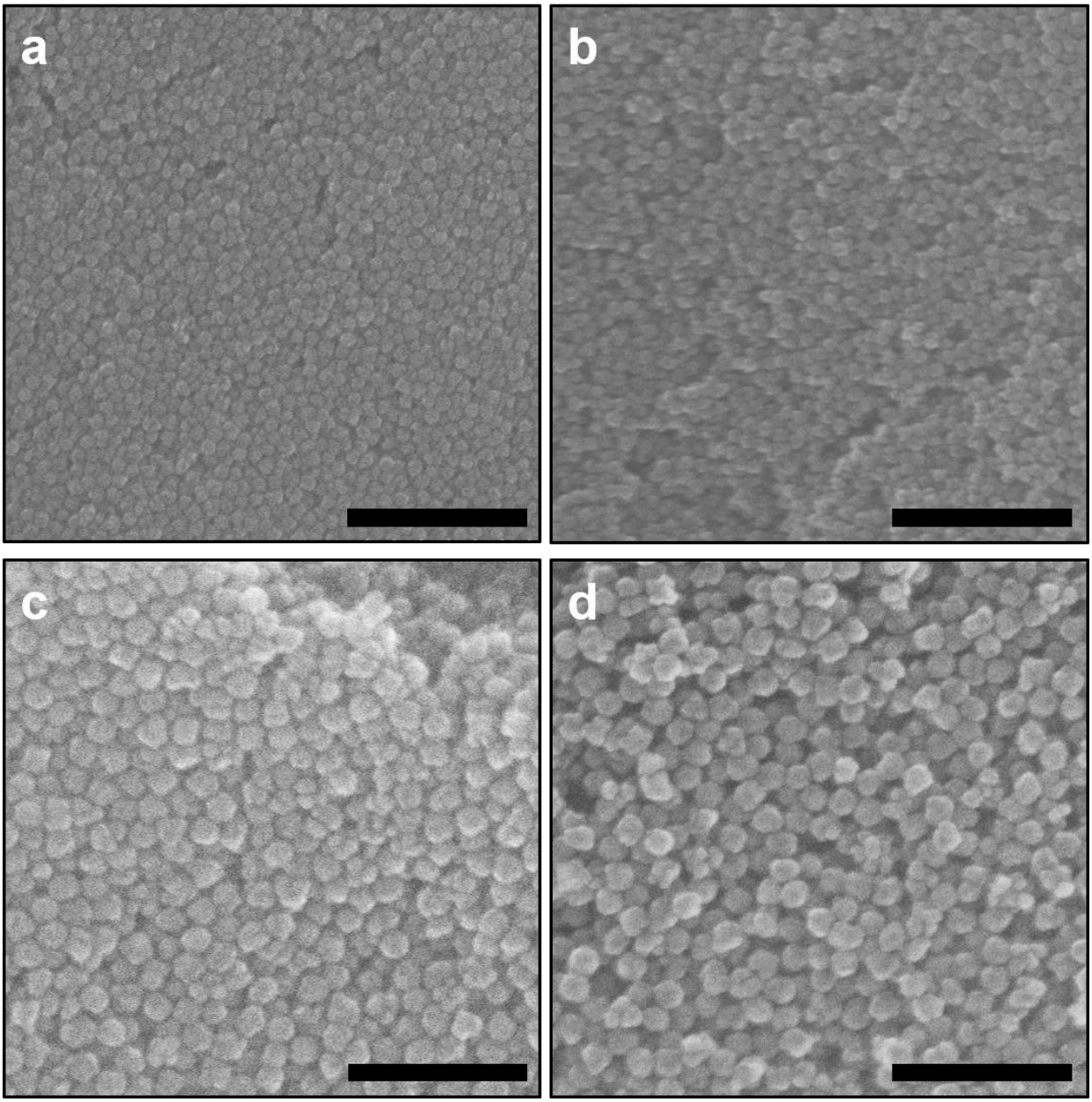

Figure S20. Scanning electron microscopy (SEM) of ITO-C (a, c) and ITO-S (b, d) films. Scale bars are 200 nm (a, b) and 100 nm (c, d).

Table S3. Surface tension properties of liquids, contact angles, and variables calculated from those values for linear regression using OWRK model.

Sample	Liquid	γ_{lv}^{P} (mN/m)	γ_{lv}^{D} (mN/m)	**X (unitless)**	Contact angle (deg)	cos(theta)	**Y (mN/m)^0.5**
ITO-C	Water	43.7	29.1	1.225	75	0.259	8.494
					79.5	0.182	7.977
					77.7	0.213	8.185
	Diiodo-methane	2.6	47.4	0.234	54.4	0.582	5.745
					50.6	0.635	5.936
					58	0.530	5.555
ITO-S	Water	43.7	29.1	1.225	26.5	0.895	12.786
					27.3	0.889	12.744
					28.7	0.877	12.666
	Diiodo-methane	2.6	47.4	0.234	23	0.921	6.974
					25	0.906	6.922
					26.8	0.893	6.872

Table S4. Linear regression results and calculated surface energies for ITO-C and ITO-S films.

Sample	Slope (mN/m)^0.5	Y-int (mN/m)^0.5	Surface Energy (mN/m)
ITO-C	2.50 ± 0.19	5.16 ± 0.17	32.9 ± 1.9
ITO-S	5.86 ± 0.05	5.55 ± 0.04	65.2 ± 0.7

References:

1 B. Tandon, S. L. Gibbs, B. Z. Zydlewski, and D. J. Milliron, Chem. Mater., 2021, 33, 6955-6964.

2 E. L. Runnerstrom, G. K. Ong, G. Gregori, J. Maier, and D. J. Milliron, *J. Phys. Chem. C*, 2018, **122**, 13624-13635.

3 L. De Trizio, R. Buonsanti, A. M. Schimpf, A. Llordes, D. R. Gamelin, R. Simonutti, and D. J. Milliron, *Chem. Mater*., 2013, **25**, 3383-3390.

4 B. H. Kim, C. M. Staller, S. H. Cho, S. Heo, C. E. Garrison, J. Kim, D. J. Milliron, *ACS Nano*, 2018, **12**, 3200-3208.

5 D. K. Owens, R. C. Wendt, *J. Appl. Polym. Sci.*, 1969, **13**, 1741-1747.

6 M. Annamalai, K. Gopinadhan, S. A. Han, S. Saha, H. J. Park, E. B. Cho, B. Kumar, A. Patra, S.-W. Kim, T. Venkatesan, *Nanoscale*, 2016, **8**, 5764-5770.

7 J. Li, H. C. Zeng, *Chem. Mater.*, 2006, **18**, 4270-4277.

8 J. L. Peters, J. C. van der Bok, J. P. Hofmann, D. Vanmaekelbergh, *Chem. Mater*, 2019, **31**, 5808-5815

9 L. Wang, Y. Dong, T. Yan, Z. Hu, A. A. Jelle, D. M. Meira, P. N. Duchesne, J. Y. Y. Loh, C. Qiu, E. E. Storey, Y. Xu, W. Sun, M. Ghoussoub, N. P. Kherani, A. S. Helmy, G. A. Ozin, *Nat. Commun.*, 2020, **11**, 2432.

10 J.-C. Dupin, D. Gonbeau, P. Vinatier, A. Levasseur, *Phys. Chem. Chem. Phys.*, 2000, **2**, 1319-1324.

11 E. L. Runnerstrom, A. Bergerud, A. Agrawal, R. W. Johns, C. J. Dahlman, A. Singh, S. M. Selbach, D. J. Milliron, *Nano Lett.*, 2016, **16**, 3390-3398.
12 E. Bêche, P. Charvin, D. Peranau, S. Abanades, G. Flamant, *Surf. Interface Anal.*, 2008, **40**, 264-267.
13 J. Stoch, J. Gablankowska-Kukucz, *Surf. Interface Anal.*, 1991, **17**, 165-167.